published in Journal of Geophysical research, **102**, 7225-7236 (1997)

Laboratory Experiments on Shear Alfvén Waves, and their Relationship to Space Plasmas.

Walter Gekelman, Stephen Vincena, David Leneman, James Maggs

UCLA Department of Physics, 1000 Veteran Avenue, Los Angeles, California 90095-1696*

Abstract

Alfvén waves are ubiquitous in space plasmas and are the means by which information about changing currents and magnetic fields are communicated. Shear Alfvén waves radiated from sources with cross field scale size on the order of the electron inertial length, $\delta = c/\omega_{pe}$, have properties which differ considerably from planar Magneto-hydrodynamic waves. Currents of cross field size , δ, are common in space plasmas. A series of experiments in the **La**rge **P**lasma **D**evice at UCLA is presented which illustrate that waves generated by small scale fluctuating currents have a parallel electric field, and radiate across magnetic field lines. Data and theory are presented for varying plasma collisionality and ratio of Alfvén speed to electron thermal velocity. Waves generated by two sources are observed to constructively interfere to produce large magnetic fields in spaital regions away from source field lines. The shear Alfvén wave is important in the Earth's auroral regions and may play a role in auroral dynamics.

* Work supported by the Office of Naval Research and the National Science Foundation

I. Introduction

Alfvén waves play a central role in the dynamics of many space plasmas from the solar corona to planetary ionospheres. They are low frequency waves (below the ion cyclotron frequency) propagating in a magnetized conducting fluid, such as the plasmas found in space. These waves not only transport electromagnetic energy but communicate information concerning changes in plasma currents and magnetic field topology. Ever since Hannes Alfvén [1942] introduced the concept of electromagnetic signals propagating through a perfect conductor these waves have attracted the interest of researchers in Physics and Geophysics. There are two very different modes of electromagnetic propagation at low frequencies, a compressional wave in which density and field strength vary and a shear wave in which only the direction of the magnetic field changes. In this paper we are concerned only with the shear Alfvén wave. In the standard MHD (Magneto-Hydro-Dynamic) picture the shear Alfvén wave is particularly interesting because wave energy is transported directly along field lines. Measurements of fluctuations in the magnetic field due to the shear Alfvén wave then give a direct map of the source of the wave. This picture is modified, however, when the source radiating the wave has physical dimensions across the magnetic field on the order of the collisionless electron skin depth, $\delta = c/\omega_{pe}$ (c is the speed of light and ω_{pe} is the electron plasma frequency).

We are not considering the compressional wave in this work. It is a spherical wave which propagates both below and above the ion gyrofrequency. The pure MHD wave dispersion, $\frac{\omega}{k} = V_A$ indicates that at frequencies below ω_{ci} the wave is cut off in the LAPD device. The shear

wave in these experiments has perpendicular wavelengths which are much smaller than the plasma column diameter. The lowest frequency shear waves are limited by the ten meter plasma column length. Longer wavelengths have been observed as column eigenmodes [Maggs and Morales, 1996] but are not discussed in this paper.

Even though Alfvén waves are a very common feature of space plasmas, obtaining a spatial picture of Alfvén wave radiation using spacecraft data is difficult because the waves are slowly varying temporally and have very long (typically thousands of kilometers) wavelengths along the magnetic field. The measurement is even more difficult if the radiation is from a small source because of problems with temporal and spatial aliasing. On the other hand, a suitably dense, magnetized laboratory plasma provides an excellent means of obtaining a spatial picture of Alfvén wave radiation patterns. The purpose of this paper is to acquaint the reader with the propagation properties of shear Alfvén waves radiated from small sources as measured in a laboratory plasma.

The properties of Alfvén waves have been the subject of several laboratory investigations. The first experiments on Alfvén waves were performed in pinches and arcs which produce high density plasmas, but suffer from high noise levels, large shot to shot variability and high collision rates. Despite these difficulties many of the basic properties of the Alfvén modes have been studied and verified in these plasmas. The first experimental evidence for the existence of Alfvén waves appeared ten years after Alfvén predicted their existence. A standing wave of the appropriate frequency was observed by Bostick and Levine [1952] in a pulsed toroidal device. Subsequent experiments in toroidal [Jephcott, 1959], and linear devices [Sawyer, et al., 1959; Wilcox, et al., 1960]

measured the wave phase velocity from the phase shift of detected wave magnetic fields, and verified its dependence on magnetic field strength and plasma density. The dispersion of the shear wave was measured by Jephcott and Stocker [1962] in a cylindrical column. The results compared favorably with a theory by Woods [1962] which included boundary conditions and collisional damping by neutrals. The properties of bounded Alfvén modes have been studied in fusion related and basic physics experiments [Cross and Lehane, 1967a, 1967b; Lehane and Paoloni, 1971; Muller, 1973]. Recent studies of both the shear and compressional mode were done in a narrow, partially ionized column by Amagishi, et al. [1989, 1990]. Wave propagation and polarization were measured but damping by neutral particles was found to significantly change the dispersion from the fully ionized case.

While these experiments establish the validity of the standard MHD picture of Alfvén waves, they do not address Alfvén wave radiation by small sources. A series of experiments on the propagation of the shear Alfvén wave launched by a small disk exciter has recently been reported by Gekelman, et al. [1994]. Related experiments using localized sources were performed by Cross in a linear machine [Cross, 1983] and Borg and Cross [1987] in a small Tokamak. These experiments differ from those reported by Gekelman in that they were performed in plasmas with high electron-neutral collisionality. The experimental results reported here establish two important new characteristics associated with Alfvén wave radiation from small sources. The first property is the spreading of radiation across magnetic field lines along trajectories called Alfvén wave cones. The second feature is a magnetic field-aligned electric field which leads to wave dissipation through resonant wave-particle interactions.

These findings bear directly upon those space plasma processes which involve field-aligned currents, fluctuating at frequencies below the ion cyclotron frequency, with cross-field scale lengths on the order of the electron skin depth. These types of situations can be expected to be found in boundary regions or regions where the plasma density or magnetic field configuration is changing rapidly in space. Examples of such regions are the magnetopause, the plasma sheet boundary layer, and the auroral current regions. Recently the Freja satellite (Lundin et. al., 1994a) has observed what its team calls Solitary Kinetic Alfvén Wave Structures (SKAWS). These waves are structured at the electron inertial length and could be directly related to the results reported here. Indeed low frequency fluctuations in the magnetic field that have been interpreted as Alfvén waves have been observed by a sounding rocket [Boehm, et al., 1990] and satellites [Chmyrev, et al., 1988; Lundin, et al.,1994b]. These observations have been associated with short scale length, cross-field density gradients and electron precipitation. Large changes in the flux of precipitating auroral electrons very commonly occur on scale lengths comparable to the electron skin depth [Borovsky, 1993]. These narrow current channels are potential sources of Alfvén wave radiation [Maggs and Morales, 1996].

II. Properties of the Shear Alfvén Wave

The shear Alfvén wave propagates with the wave magnetic field vector perpendicular to the background field. The dispersion relation for this wave can be obtained by combining the two Maxwell equations for the curl of the electric and magnetic field. These equations result in the wave equation for a plane wave propagating in a spatially uniform plasma,

$$\mathbf{k} \times \mathbf{k} \times \mathbf{E} + \frac{\omega^2}{c^2} \varepsilon \cdot \mathbf{E} = 0 \qquad (1)$$

where **E** is the electric field vector, ε the dielectric tensor, **k** the wave number vector, and ω the angular frequency. For the shear Alfvén wave, the electric field and wave number vector are co-planar, so we can write the wave dispersion relation, using Eq. 1, as

$$\varepsilon_{\parallel} (k_{\parallel}^2 - \frac{\omega^2}{c^2} \varepsilon_{\perp}) = -k_{\perp}^2 \varepsilon_{\perp} \qquad (2)$$

where the subscripts ∥ and ⊥ refer to components of quantities along and across the background magnetic field respectively. In the shear Alfvén wave the current along the magnetic field is carried by electrons while the current across the magnetic field is carried by ions (due to the ion polarization drift). In addition the displacement current is negligible so that the components of the dielectric tensor can be written

$$\varepsilon_{\parallel} = -\frac{\omega_{pe}^2}{\omega^2} \zeta^2 Z'(\zeta) \quad ; \quad \varepsilon_{\perp} = \frac{-\omega_{p+}^2}{\omega^2 - \Omega_+^2} \frac{(1 - e^{-\lambda_+} I_0(\lambda_+))}{\lambda_+} \qquad (3)$$

where ω_{p+} and Ω_+ are the ion plasma frequency and gyrofrequency, and where $\zeta = \omega/k_{\parallel}a$ and $\lambda_+ = (k_{\perp}a_+/\Omega_+)^2$. The average electron thermal speed is denoted by $a = (2T_e/m_e)^{1/2}$ with T_e the electron temperature, measured in ergs, and m_e the electron mass. The ion thermal velocity a_+ is defined similarly with T_+ and M_+ denoting the ion temperature and mass. $Z'(\zeta)$ is the derivative of the plasma dispersion function with respect to ζ and I_0 is the modified Bessel function of order zero. In a plasma where the ion

temperature is much smaller than the electron temperature ($T_+ << T_e$) Eq. 2 can be written, using Eq. 3, as

$$Z'(\zeta)\,(s^2(1-\varpi^2)-\zeta^2) \;=\; k_\perp^2\,\delta^2 \qquad (4)$$

where $s = v_A/a$ is the ratio of the Alfvén velocity ($v_A = \sqrt{B^2/(4\pi n m_+)}$) to the electron thermal speed, and ϖ is the normalized angular frequency ($\varpi = \omega/\Omega_+$).

Eq. 4 describes propagation of the shear Alfvén wave in the general case, but much can be learned by analyzing the two limiting cases of large and small Alfvén speed, $s^2 >> 1$ and $s^2 << 1$. The parameter s^2 is related to the electron plasma beta, $\beta_e = (\frac{8\pi nkT}{B^2})$, as:

$$s^2 \;=\; \frac{v_A^2}{a^2} \;=\; \frac{m_e}{M_+}\frac{1}{\beta_e} \qquad (5)$$

Thus in the case that s^2 is large, the Alfvén speed is larger than the electron thermal speed and the electron plasma beta is less than the mass ratio. In this case ($s^2 >> 1$) we may analyze Eq. 4 by assuming that ζ is large (i.e., the wave phase velocity along the magnetic field is much larger than the electron thermal speed) and use the asymptotic expansion of the derivative of the plasma dispersion function $Z' = 1/\zeta^2$. Eq. 4 then gives the dispersion relation:

$$\frac{\omega^2}{k_\parallel^2} \;=\; \frac{v_A^2(1-\varpi^2)}{(1+k_\perp^2\delta^2)} \qquad (v_A^2 >> a^2) \qquad (6)$$

This dispersion relation describes the propagation of what is commonly referred to as the inertial Alfvén wave. The perpendicular group velocity for the inertial Alfvén wave is in the negative $k_\perp$ direction. That is, the wave is a backward wave for propagation across the magnetic field. In the limits of $k_\perp$ -> 0, and ϖ -> 0 (or $\omega << \omega_{ci}$) the dispersion relation reduces to the standard MHD dispersion relation. The inclusion of non-zero values of $k_\perp$ results in two important consequences, a spreading of wave energy across magnetic field lines and a non-zero parallel electric field. The two-dimensional formulation presented here corresponds to cylindrical symmetry, and we can associate $k_\perp$ with a radial coordinate, r, and $k_\parallel$ with an axial coordinate, z. The corresponding second-order partial differential equation obtained from Eq. 6 by substituting $k_\parallel \rightarrow i\frac{\partial}{\partial z}$ and $k_\perp \rightarrow i\frac{\partial}{\partial r}$ has the characteristics $\frac{dr}{dz} = \pm\frac{k_A\,\delta}{(1-\varpi^2)^{1/2}}$. Thus the inertial Alfvén wave propagates along trajectories that form an angle to the background magnetic field. This propagation property is referred to as propagation along Alfvén wave cones. The component of the electric field parallel to the magnetic field is related to the perpendicular component by

$$E_\parallel = \frac{k_\parallel k_\perp}{k_\perp^2 - (\omega/c)^2\varepsilon_\parallel} E_\perp = \frac{k_\parallel k_\perp \delta^2}{1+k_\perp^2\delta^2} E_\perp = \frac{k_A k_\perp \delta^2}{(1-\varpi^2)^{1/2}(1+k_\perp^2\delta^2)^{1/2}} E_\perp \quad (7)$$

where $k_A = \omega/v_A$. Thus the parallel electric field for large $k_\perp\delta$ (short perpendicular wavelengths) is $E_\parallel = (k_A\delta)E_\perp/(1-\varpi^2)^{1/2}$.

In the other limiting case of small s^2 ($v_A^2 << a^2$), the plasma electron beta is larger than the mass ratio and the Alfvén speed is much slower than the electron thermal speed. In this case the electrons respond adiabatically to the wave field and we may approximate the derivative of the plasma

dispersion relation with its value for small ζ, or Z' = -2.0. Eq. 4 then gives the dispersion relation

$$\frac{\omega^2}{k_{\|}^2} = v_A^2 (1 - \varpi^2 + k_{\perp}^2 \rho_s^2) \qquad (v_A^2 << a^2) \qquad (8)$$

where ρ_S is the ion sound gyroradius, $\rho_S = c_S/\Omega_+$, with $c_S = (T_e/M_+)^{1/2}$ the ion sound speed. This dispersion relation describes the propagation of the so called kinetic Alfvén wave. Once again the standard MHD dispersion relation is recovered in the case $k_\perp = 0$, and $\varpi \approx 0$. The perpendicular group velocity for the kinetic Alfvén wave is in the positive $k_\perp$ direction. Thus the kinetic Alfvén wave is a forward wave across the magnetic field in contrast to the inertial Alfvén wave. The phenomena of Alfvén wave cones does not exist for the kinetic Alfvén wave. The partial differential equation corresponding to the dispersion relation given by Eq. 8 is fourth order, indicating that the propagation pattern associated with the kinetic Alfvén wave is more complicated than for the inertial Alfvén wave. The kinetic Alfvén wave has a field aligned component of the electric field related to the perpendicular component by

$$E_{\|} = \frac{-k_{\|} k_{\perp} \rho_s^2}{1 - \varpi^2} E_{\perp} = \frac{-k_A k_{\perp} \rho_s^2}{(1 - \varpi^2)(1 - \varpi^2 + k_{\perp}^2 \rho_s^2)^{1/2}} E_{\perp} \qquad (9)$$

For $k_\perp \rho_S$ large the parallel electric field is $E_{\|} = -(k_A \rho_S) E_\perp / (1 - \varpi^2)$.

The two limiting cases of the kinetic and inertial Alfvén waves demonstrate that the propagation properties of the Alfvén wave across the magnetic field strongly depend upon the value of $\zeta = \omega/k_{\|}a$, and thus electron plasma beta. While the two limiting cases are useful in illustrating some of the properties of the Alfvén wave, the general case must be treated

by using a full kinetic treatment for the electron dynamics as indicated in Eq. 4.

III. Experimental Arrangement

Experiments on Alfvén wave propagation were conducted in the LAPD (LArge Plasma Device) [Gekelman, et al. ,1991] at UCLA (University of California, Los Angeles). The LAPD is a large cylindrical stainless steel chamber one meter in diameter, ten meters long, surrounded by 68 pancake magnets. The machine is ideal for studying Alfvén waves because of its large physical size, dense plasma and substantial magnetic field. The LAPD plasma column is 50 cm in diameter and 9.4 meters in length. The experiments reported here were performed in a He plasma with a uniform 1.1 kG magnetic field at densities ranging from 1.0 to 2.5×10^{12} cm^{-3}. Plasma densities are measured using both Langmuir probes and a 70 GHz microwave interferometer.

The LAPD plasma is produced by a DC (direct current) discharge using an oxide (BaO) coated nickel cathode. The chamber is filled with helium neutrals at a pressure of $2. \times 10^{-4}$ Torr. Plasma is produced by pulsing the cathode negative ($\approx$100 V) with respect to a wire mesh anode located 60 cm from the cathode. The discharge pulse is repeated at a rate of 1 Hz to allow for efficient signal averaging and data processing. The discharge pulse typically lasts 5-10 ms after which it is terminated. The termination phase of the pulse lasts about 0.5 ms during which the negative bias on the cathode rises slowly. In the termination phase the plasma density and temperature slowly decrease from their peak values achieved during the discharge. The termination phase ends when the negative voltage pulse to the cathode is completely terminated at which point the plasma afterglow

phase begins. During the afterglow phase the temperature falls rapidly while the density continues to decay slowly. Plasma temperatures of about 10 eV are achieved during the discharge and the temperature is about 2-3 eV at the end of the termination phase. The plasma temperature is measured using a Langmuir probe. Some of the experiments reported here were conducted in the termination phase of the discharge and others during the active discharge.

Figure 1 shows the experimental setup for launching and detecting the shear Alfvén wave.

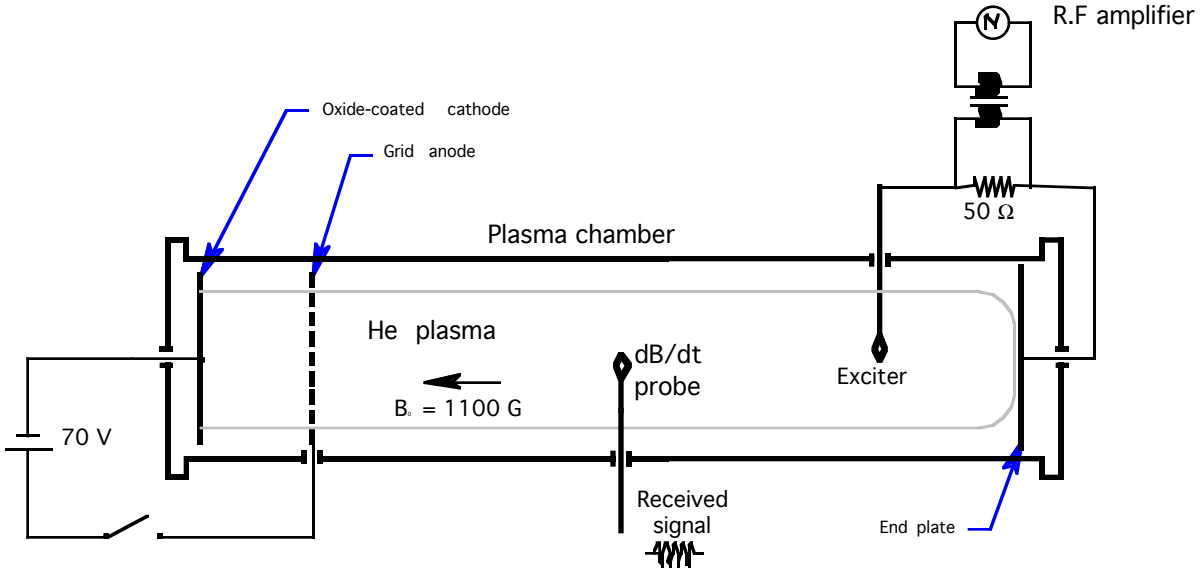

FIGURE 1) Schematic of the experimental set-up showing cathode, at distance δz = 60 cm from a gridded anode and the floating end plate of the machine (δz = 10 m). In this view a single disk exciter for the shear wave is fed via a transformer. The disk may be biased with a capacitor in series with a transistor switch. Data is acquired by a three-axis induction coil, magnetic probe which may be inserted at a number of locations along z. In the wave interference experiments two identical wave launchers are employed.

The radially movable antenna is a circular disk of wire mesh (transparency ≈ 50%) attached to the inner conductor of a coaxial cable. The outer conductor is isolated from the plasma and the support is made of glass. The antenna is mounted on a bellows to allow for freedom in positioning. The radiated wave magnetic field is measured in planes perpendicular to the background magnetic field at various axial positions away from the antenna using a triaxial induction loop probe. The magnetic probe consists of three orthogonally oriented,
8 mm diameter, 3 mm thick, 58 turn, differential current loops. The magnetic probe was calibrated by measuring, in air, the magnetic field surrounding a long straight wire modulated at 300 kHz.

To excite the waves, a phase locked RF (Radio Frequency) tone burst is fed to the disk exciter through a broadband amplifier and isolation transformer. As shown in Figure 1, the signal ground is referenced with respect to an electrically floating Cu plate terminating the plasma column. The modulated grid potential drives a field aligned RF current which excites Alfvén waves. Current must flow in and out of the disk antenna. If the disc is at floating potential the current consists of electrons on one half cycle and ions on the next. Modulation of an electrically floating grid limits the amplitude of waves because the amount of ion current that can be drawn from the plasma is limited. Large amplitude waves can be launched by positively biasing the antenna, drawing electron saturation current, and then modulating that current ($V_{bias} > V_{peak\text{-}rf}$). Since a biased exciter draws a current which results in depletion of the density along the flux tube threading the antenna, the bias is applied with a pulsed transistor switch only during the time the RF is present.

A wide range of values for the background magnetic field strength, density and electron temperature are achievable in the plasmas produced with the LAPD. Therefore experiments are possible over a considerable range of electron beta values around the mass ratio. This flexibility allows us to investigate the properties of the Alfvén wave between the inertial and kinetic Alfvén wave limits. For example, during the discharge phase of LAPD plasmas a typical value of the density is 2. x 10^{12} cm^{-3} with an electron temperature of 10 eV, corresponding to an electron beta of 3.2 x 10^{-3} in a 500 Gauss field to 2. x 10^{-4} in a 2000 Gauss field. In a Helium plasma the electron to ion mass ratio is 1.36 x 10^{-4}, so that electron beta values in the discharge plasma are generally above the mass ratio (i.e., in the kinetic Alfvén wave regime). In the afterglow phase of the plasma a typical density is 2. x 10^{11} cm^{-3} with an electron temperature of 0.5 eV corresponding to an electron beta of 1.6 x 10^{-5} at 500 Gauss to 1. x 10^{-6} at 2000 Gauss. These values are below the mass ratio, so that the afterglow plasma is representative of the inertial Alfvén wave case.

An effect which must be considered in dealing with low frequency waves is the collisionality of the plasma. Collisions become important when $k_{\|}\lambda_{mfp}$ is of order unity or less (λ_{mfp} is the mean free path). This criteria depends upon the wave frequency, plasma temperature and the type of collision process considered. In the LAPD, collisions of electrons with Helium neutrals is negligible because the plasma is highly ionized [Maggs, et al., 1991]. Electron-ion Coulomb collisions, on the other hand, are an important effect because the LAPD plasmas are dense and not very hot (due to the limited energy confinement time in a linear device). The electron-ion Coulomb collision frequency is [Koch and Horton, 1975]

$$\nu_e = \frac{\pi}{\sqrt{2}} \frac{n_e e^4 \ell n\Lambda}{m_e^{1/2} T_e^{3/2}} \qquad (10)$$

where lnΛ is the Coulomb logarithm. In the typical discharge plasma the electron-ion collision frequency is about 1. x 10^6 sec^{-1}. In the afterglow plasma the collision frequency is about 1. x 10^7 sec^{-1}. Even though the density of the afterglow plasma is lower than that of the discharge plasma, the collision frequency is higher due to the lower electron temperature.

The principal effect of Coulomb collisions on the electron dynamics is scattering in pitch angle at constant energy. The changes in wave propagation caused by electron pitch angle scattering have been investigated by Koch and Horton [1975]. They give an expression for the plasma dispersion function as modified by Coulomb collisions that can be used in the dispersion relation given by Eq. 4. Interestingly pitch angle scattering reduces the collsionless dissipation (Landau damping) of propagating waves except in those regions of velocity space in which the collisionless damping is exponentially small. Reduction in dissipation occurs because electron pitch angle scattering limits the electron-wave resonance interaction time. Figure 2 illustrates the changes in the imaginary and real parts of the parallel wave number of propagating Alfvén waves due to electron pitch angle scattering for three values of ν_e/ω (0., 0.25, and 4.0). Collisions alter both the propagation properties and dissipation of the shear Alfvén wave but the general behavior of the highly collisional plasma, ν = 4.0, is surprisingly similar to the collisionless plasma ν = 0.

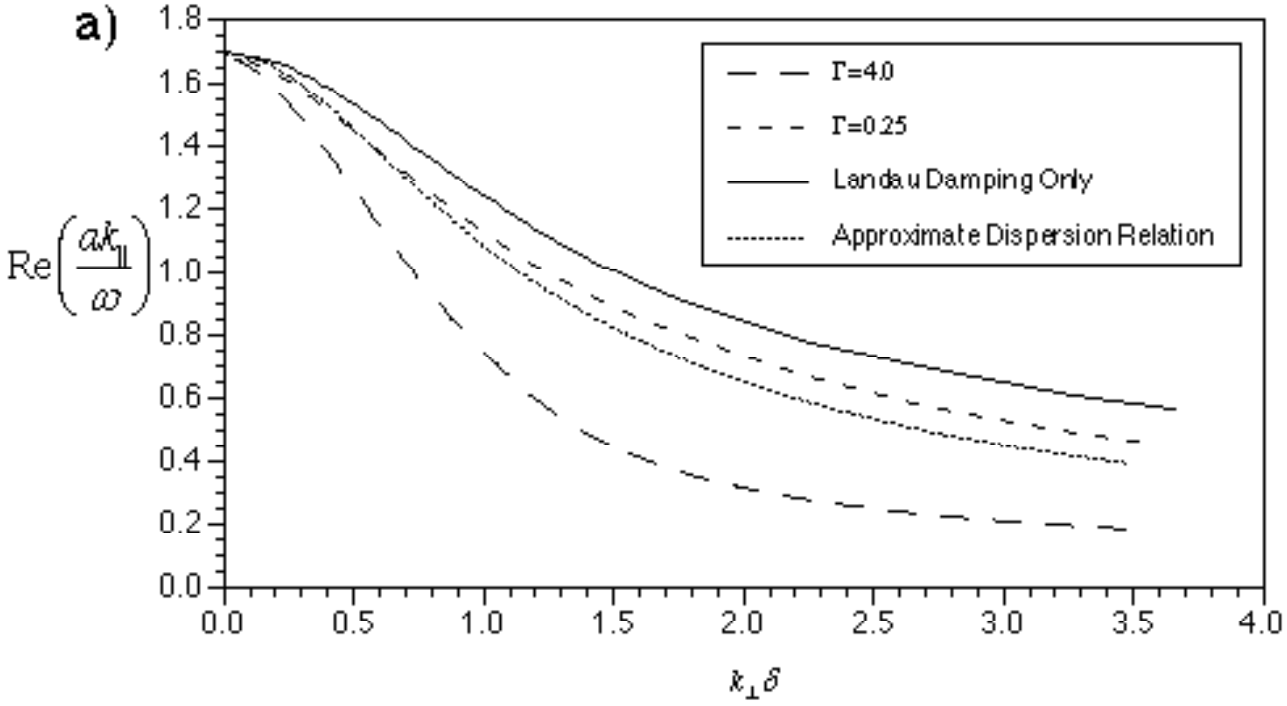

Figure 2a) The dependence of the real part of the the parallel wave number as a function of $k_{\perp}\delta$ is shown for pure Landau damping and two values of Γ for δ = 0.725 cm and ϖ = 0.6. The dependence given by the approximate kinetic Alfvén wave dispersion relation, Eq. 8, is shown for comparison.

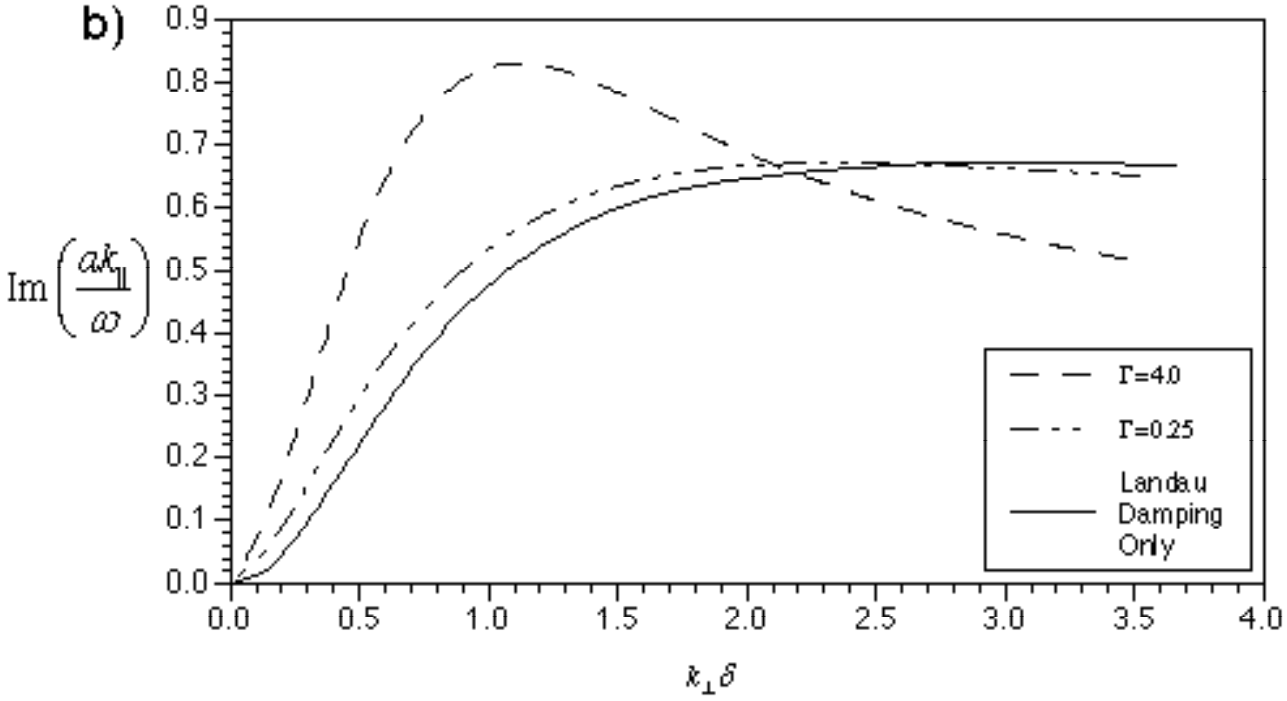

Figure2b) The imaginary part of the parallel wave number as a function of $k_\perp\delta$ for pure Landau damping, $\Gamma = 0.25$ and $\Gamma = 4.0$. Electron pitch angle scattering from Coulomb collisions actually reduces wave dissipation for $k_\perp\delta$ values larger than about 2.5.

Coulomb collisions are not generally an important process in space plasmas, but electron pitch angle scattering can be. For example, in the auroral ionosphere, the presence of electrostatic turbulence in the whistler frequency band can lead to strong electron pitch angle scattering. The effects of electron pitch angle scattering on Alfvén wave propagation are the same whether due to Coulomb collisions or electrostatic turbulence. Thus, investigating Alfvén wave propagation in the LAPD in the presence of pitch angle scattering is relevant to the space plasma environment. While propagation of Alfvén waves in a collisionless plasma can not be investigated in the LAPD, a wide range of plasma betas and pitch angle scattering environments are accessible.

A simplified method for modeling collisions is to introduce a Krook collision term into the linearized Vlasov equation. The dispersion relation (Eq 4) then becomes

$$Z'(\eta)(1+i\Gamma)\left[\, s^2(1-\varpi^2) - \zeta^2 \right] \;=\; k_\perp^2\,\delta^2 \qquad (11)$$

where $\eta = \zeta(1+i\Gamma)$, $\Gamma = \nu_{collisions}/\omega$, and the derivative of Z is now taken with respect to η.

IV. Experimental Results

1. Expected Behavior

The shear Alfvén wave transports energy directly along the magnetic field (no perpendicular group velocity) if $k_\perp$ is zero. For non-zero $k_\perp$ magnetic energy is transported across the magnetic field. The amplitude of radiation generated at a particular $k_\perp$ depends upon the size of the source radiating the wave. Small sources radiate more energy across the magnetic field than large sources. A large source is one with a physical size in the direction across the magnetic field much larger than the electron skin depth, δ, while a small source is one with physical size on the order of δ. A large source produces wave energy at small values of $k_\perp$ ($k_\perp\delta << 1$), while a small source radiates waves at large values of $k_\perp$ ($k_\perp\delta \approx 1$).

In the experiments reported here, Alfvén waves were radiated using small sources consisting of semi-transparent wire mesh disks with radii on the order of δ. Assuming azimuthal symmetry, the magnetic field radiated from these wire mesh antennas has only a component in the azimuthal direction, $\vec{B} = B_\theta(r,z)\,\hat{e}_\theta$. The spatial dependence of the radiated magnetic field is given by an integral expression involving the first order Bessel function J_1 [Morales, et al.,1994],

$$B_\theta(r,z) = \frac{2I_0}{cr_d}\int_0^\infty dk_\perp \frac{\sin(k_\perp r_d)}{k_\perp} J_1(k_\perp r)\exp\left(i k_\parallel(k_\perp) z\right) \qquad (12)$$

where I_0 is the oscillating current to the disk antenna and the disk radius is denoted by r_d. The dependence of parallel wave number on perpendicular wave number (i.e., $k_\parallel(k_\perp)$) is found by solving the dispersion relation given in Eq. 4. Examples of such solutions are illustrated in Fig. 2.

As noted above, in the inertial Alfvén wave limit the wave propagates along Alfvén wave cones. This means that the oscillating plasma currents

associated with the shear wave radiation are contained within cones emanating from all points around the edge of the disk antenna as illustrated (in cross section) in Figure 3. The radial position of the outer edge of the cone associated with the disk edge is given by

$$r_{edge} = \frac{k_A \delta z}{\sqrt{1-\varpi^2}} + r_d \qquad (13)$$

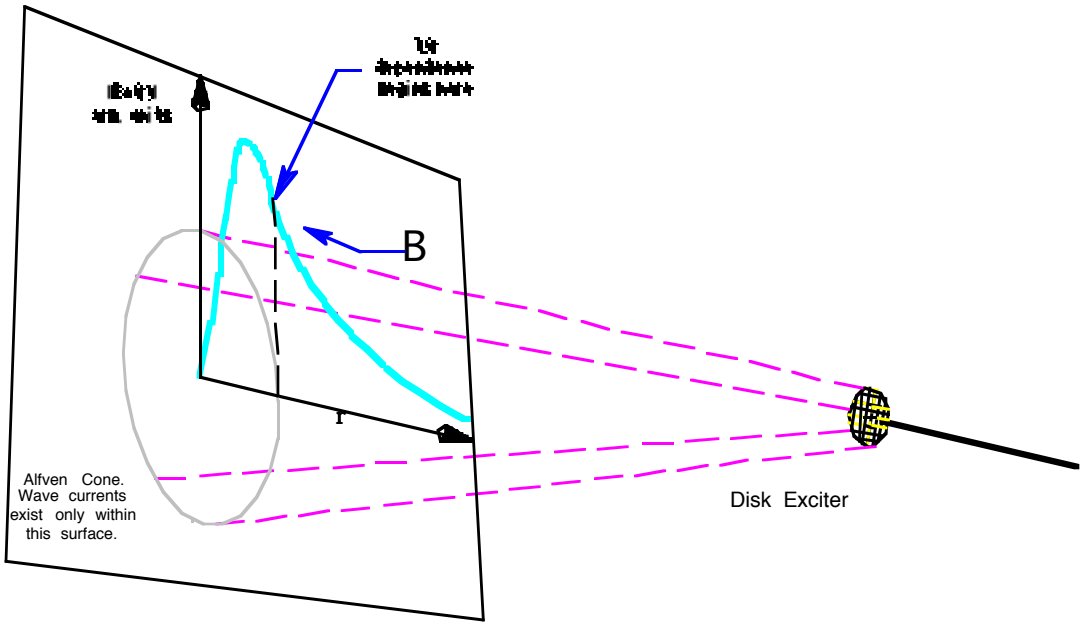

Figure 3) The geometry of Alfvén wave radiation. The wave is launched from a mesh disk exciter with $r \approx \delta$. The wave is detected on a plane several meters from the disk. The radial wave pattern $B_\theta(r)$ has a null on axis and drops off as $1/r$ where $r > r_{edge}$.

According to Eq. 12, at any fixed axial position away from the disk exciter, the expected radial profile of the magnitude of the wave magnetic field has three characteristic features. First, the field is always zero at the disk

center. Second, it increases with radial distance away from the disk center and reaches a peak value. The radial location of the peak value increases with axial distance away from the exciter. Third, upon reaching the position, r_{edge} (the location of the outer Alfvén cone), the field decreases as 1/r. The 1/r decrease outside the Alfvén cone indicates that all wave currents are contained within the cone (The oscillating wave currents are confined to $r < r_{edge}$). At a fixed radius larger than r_{edge} (i.e., outside the Alfvén cone) the magnetic field has the same value at all axial locations. In reporting our observations we compare the measured magnetic field profiles to the theoretically predicted profiles as given by Eq. 12.

2. Results

We now present our observations of the radiation of Alfvén waves from small disk antennas. Generally, we find the radiated field behaves in the expected fashion. We first present observations of Alfvén waves radiated from a single disk exciter, verifying the spreading of magnetic energy across field lines. Typically, the Alfvén wave radiation spreads slowly across the magnetic field because $k_A\delta << 1$, but wave currents and their associated magnetic fields do indeed broaden across the ambient magnetic field. This spreading can be significant at large distances from the source of excitation. Next, we present the results of radiation from multiple sources to show the effects of constructive and destructive interference on determining the wave pattern.

a) Radiation from a small disk antenna.

The magnetic field pattern of Alfvén wave radiation from a small disk antenna with radius equal to the electron skin depth was measured with electron beta both larger and smaller than the mass ratio. The antenna was

placed in the center of the plasma column and the field pattern measured in planes across the magnetic field at several axial locations. A phase locked tone burst consisting of several cycles is applied to the disk and received by a tri-axial magnetic probe. Typically, at each spatial location the received signal from each induction loop is recorded and stored on computer disk for ten to twenty plasma pulses. The probe is then moved to a new location and the process repeated.

The parallel phase velocity and dispersion of the radiation is measured by comparing the received signal at different axial locations along the same field line for several modulation frequencies. The results of such a measurement are shown in Fig. 4. Figure 4a shows the received tone burst from one of the induction loops at three axial positions (a=157 cm, b = 252 cm , c = 346 cm from the antenna). The phase delay of the wavepackets is clearly visible. The Alfvén speed in this case is 1.1×10^8 cm/sec and the electron thermal velocity 8.0×10^7 cm/sec so that this case is representative of the inertial Alfvén wave. In Figure 4b the measured wave dispersion is compared to the dispersion relation given in Eq. 6 with $k_\perp = 0$.

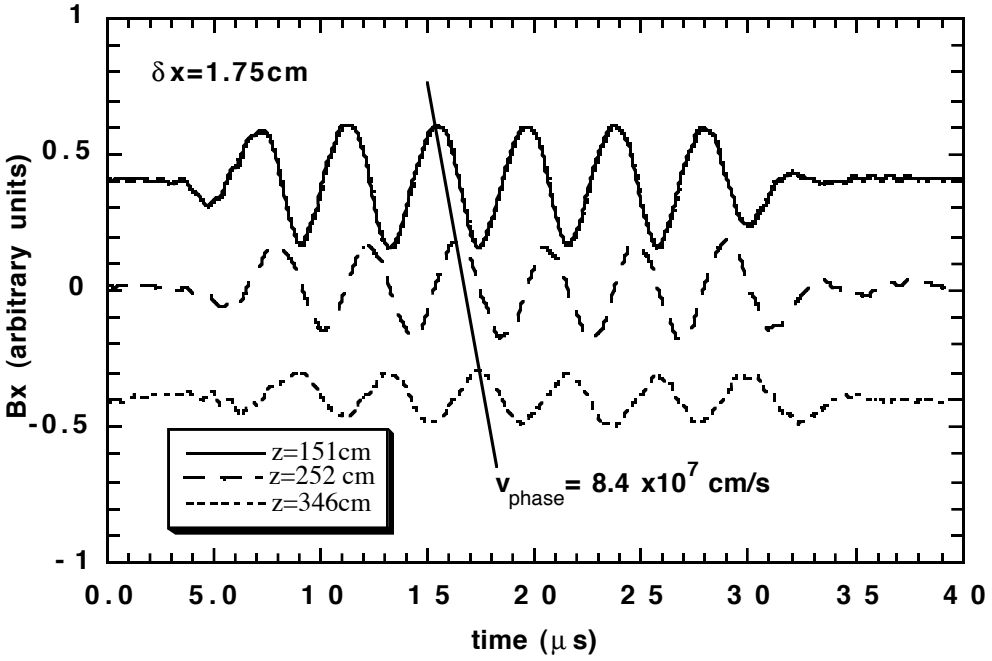

4 a) Magnetic field from a tone burst at three axial locations. Here z is the distance from the exciter to the detector and the background magnetic field B_Z = 1.1 kG. δx is the radial displacement of the field line along which measurements are taken from the center of the disk exciter.

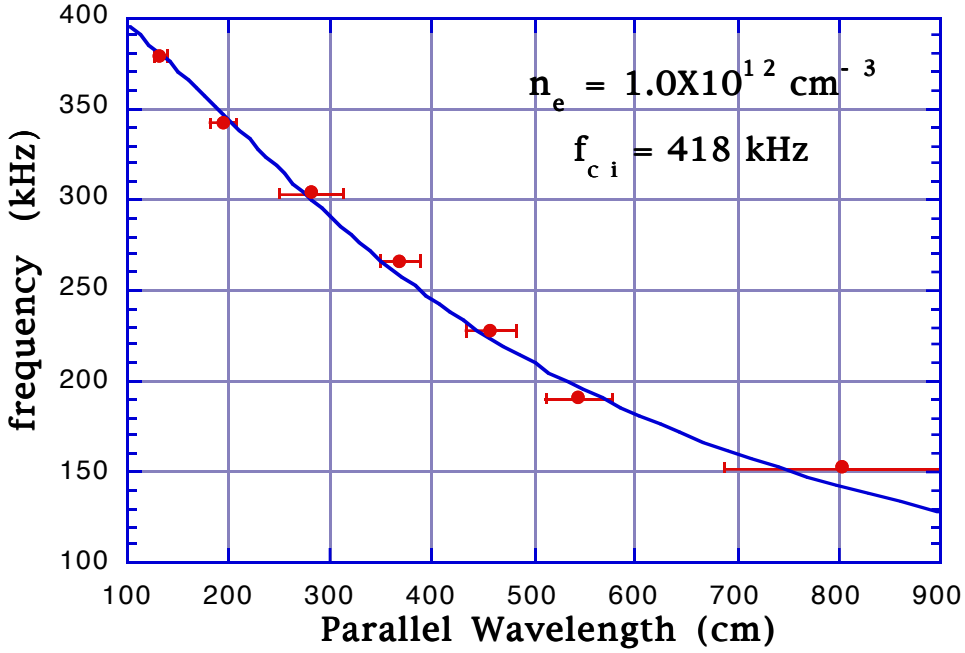

Figure 4b) Measured dispersion compared to that expected for the shear Alfvén wave. The launched wave was a tone burst as in 4a. The solid curve is a plot of equation 6 with $k_\perp \approx 0$.

The radiation pattern produced from the disk antenna is expected to be azimuthally symmetric with the magnetic field entirely in the azimuthal direction. The axial magnetic field component of the radiated field was indeed observed to be much smaller than the radial component $(\delta B_Z)/(\delta B_\theta) \approx .01)$ but departures from azimuthal symmetry were observed. To illustrate the behavior of the radiated wave magnetic field we first present a radial profile and a two dimensional vector picture of the kinetic Alfvén wave radiation before showing a three dimensional schematic of the inertial Alfvén wave.

Measurements along a radius from the center of the disk antenna of the time-averaged magnitude of the radial component of the wave magnetic field, $|B_\perp| = \sqrt{B_x^2 + B_y^2}$ are shown in figure 5.

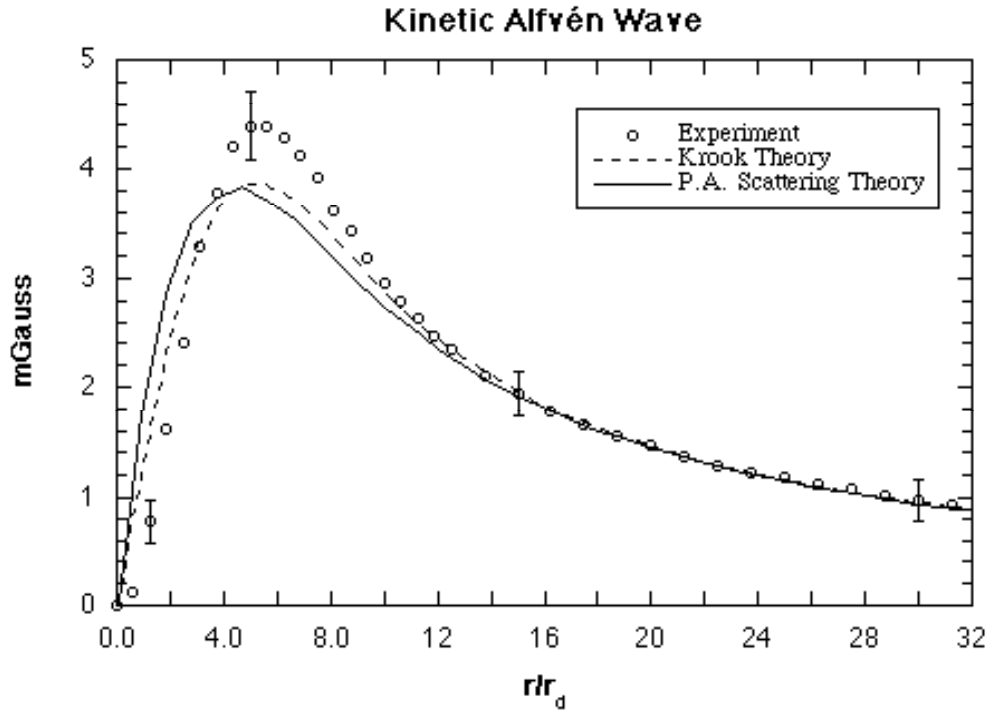

Figure 5) Radial profile of $|B_\theta|$ for a low amplitude tone burst in Helium. Kinetic shear wave at $\omega/\omega_{Ci} = 0.58$, $n_0 = 2.5X10^{12}$ cm $^{-3}$, $B_0 = 1.1$ kG and $T_e = 3.0$ e.V. The measurements are shown with open circles and two theoretical predictions with a solid and a dashed curve. The solid curve shows the field profile predicted from assuming electron pitch angle (P.A.) scattering and uses the measured values of n_0 and T_e. The dashed curve uses the Krook model of collisions and uses an ad-hoc Γ-value that gives the best fit (in this case $\Gamma = 3.25$).

A magnetic field profile for the case of the kinetic Alfvén wave ($\beta_e = 3.0 \times 10^{-4}$, $s^2 \approx 0.53$) is shown in figure 5. The probe is located 1.57 m ($\approx 0.75\ \lambda_{||}$) away from the exciter along the magnetic field. Alfvén wave cones

do not exist in the kinetic regime and the theoretical expression for the wave pattern differs from that in the inertial case. However, in practice, the two patterns have many similarities. For example, the kinetic wave pattern has a 1/r dependence at large r as predicted for the inertial case outside the Alfvén wave cones (Eq. 13). Also from Fig. 5 we see the signal is close to zero at r = 0. Furthermore the spreading of the wave magnetic field across field lines is evident in both the location of the beginning of the 1/r portion ($r/r_d \cong 8$) of the pattern and the peak amplitude of the magnetic field. The differences between the inertial and kinetic cases are most apparent at axial distances of less than one wavelength from the disk exciter. A detailed comparison of the two cases is the subject of a future paper.

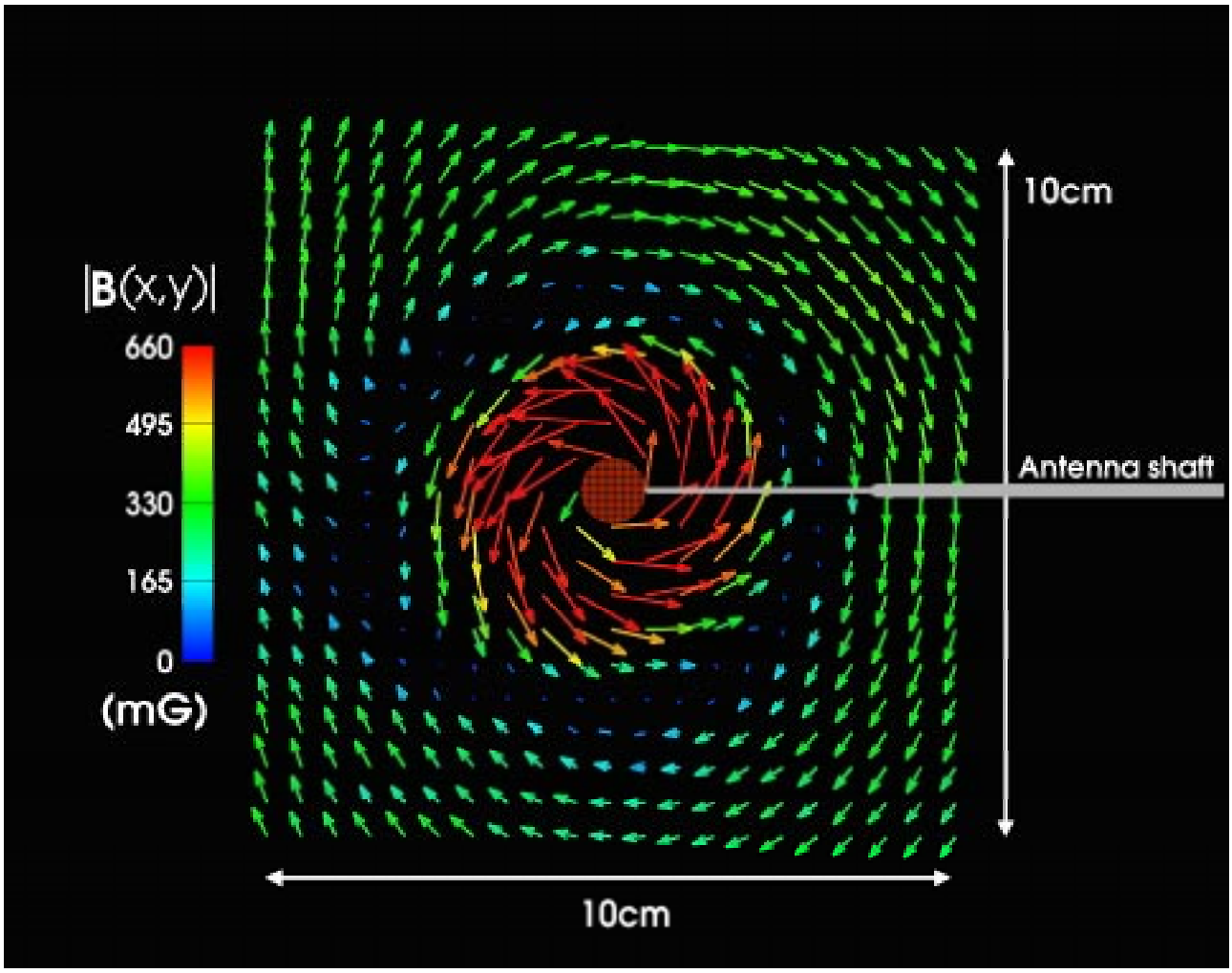

Figure 6) Measured magnetic field $B_{\perp}(x,y)$ for a wave with $\varpi = 0.77$ in a plane 1.54 meters (approximately one parallel wavelength) from the disk exciter. A scale model of the exciter is superposed on the data. The vectors are color coded in accord with their magnitude.

The two-dimensional pattern of the wave magnetic vector field is shown in Figure 6 for $\beta_e = 2.3X10^{-4}$. Instantaneous values of the perpendicular component of the wave magnetic field at 441 spatial locations in a plane perpendicular to the background magnetic field is shown for a wave with frequency, f = 320 kHz, ($\varpi = 0.77$). The wave burst

was 28 cycles long and the data shown was collected during the burst. Vectors are color-coded to aid the eye, with red denoting the largest values and blue the smallest. The largest vector in the diagram has length of 660 mG. ($B_{\perp\, max}/B_{0z}$ = 6.0X10^{-4}). Shown superimposed on the vector pattern , and to scale, is the disk antenna. The axial location of the data plane is 1.02 parallel wavelengths ($\lambda_{\parallel}$ =1.54 m) from the antenna. The planar data illustrates that the wave magnetic field exhibits a high degree of azimuthal symmetry but some departure from symmetry is evident. Wave propagation across the magnetic field is also evident from the reversal of the field direction moving radially outward from the antenna.

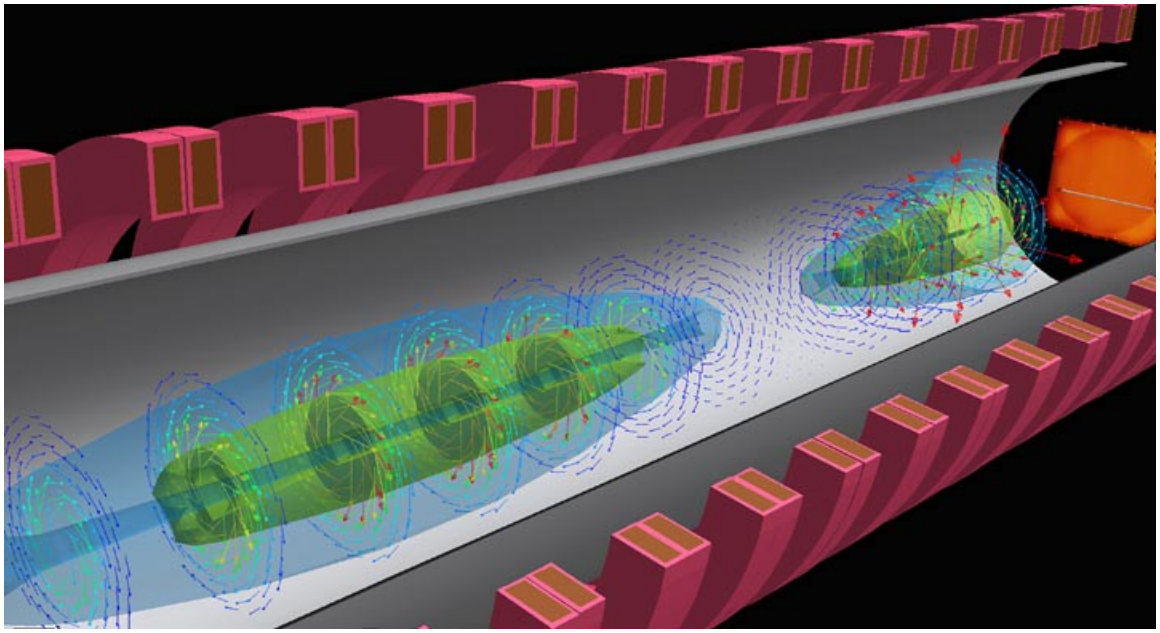

Figure 7) Composite showing a cutaway view of the LAPD device and shear Alfvén waves propagating within it. Magnets, which are colored magenta, surround the grey cylindrical vacuum vessal. The waves are shown as isosurfaces (of arbitrary field strength) and vector fields. Each structure is one half a wavelength long in the axial (z) direction and moves along z at the Alfvén speed ($\approx 10^8$

cm/sec). The wave data have been scaled by a factor of two in the radial direction for easier viewing. This was done because the cone angle is relatively small (≈ 1 degree).

In summary, to help illustrate the radiation pattern of the shear Alfvén wave in the LAPD we have calculated the theoretically expected three dimensional wave pattern ($n = 1.1 \times 10^{12}$ /cm^3, $B_0 = 1.1$ kG, f = 200 kHz, $\Gamma = 6.0$, cold plasma limit) and rendered it in Figure 7. Shown to scale is the shaft of the mesh antenna which launches the wave, the oxide coated cathode at emission temperature and a cutaway view of the magnets which surround the vacuum vessel. Superimposed on this are two cigar-like structures surrounded by vectors. These predicted patterns agree well with measured patterns on the planes over which measurements were taken. Each "cigar" is composed of two nested isosurfaces of wave magnetic field. The surfaces are contained within one half wavelength. The magnetic field is also displayed as a vector field in planes orthogonal to the background field. Fig. 6 is an example of one such plane. Note that, for the shear wave, there is no B_z component. The azimuthal wave field has a different sense of rotation for successive half wavelengths along the magnetic field. The structures depicted in Figure 7 move along the background field at the Alfvén speed. What is difficult to see in the perspective of Fig. 7 is the spreading of the wave fields across the ambient field. This effect is best illustrated using radial profiles as in Fig. 5.

b) Superposition of Alfvén wave Pulses

Propagation of Alfvén waves across the magnetic field makes nonlocal interactions between waves radiated from different sources possible as illustrated schematically in Figure 8. To investigate the interaction between

Alfvén waves, two identical disk antennas are situated in a uniform, magnetized plasma at the same axial location but on separate field lines. Each disk is excited by an RF signal coupled to the plasma through an isolation transformer to separate power amplifiers.

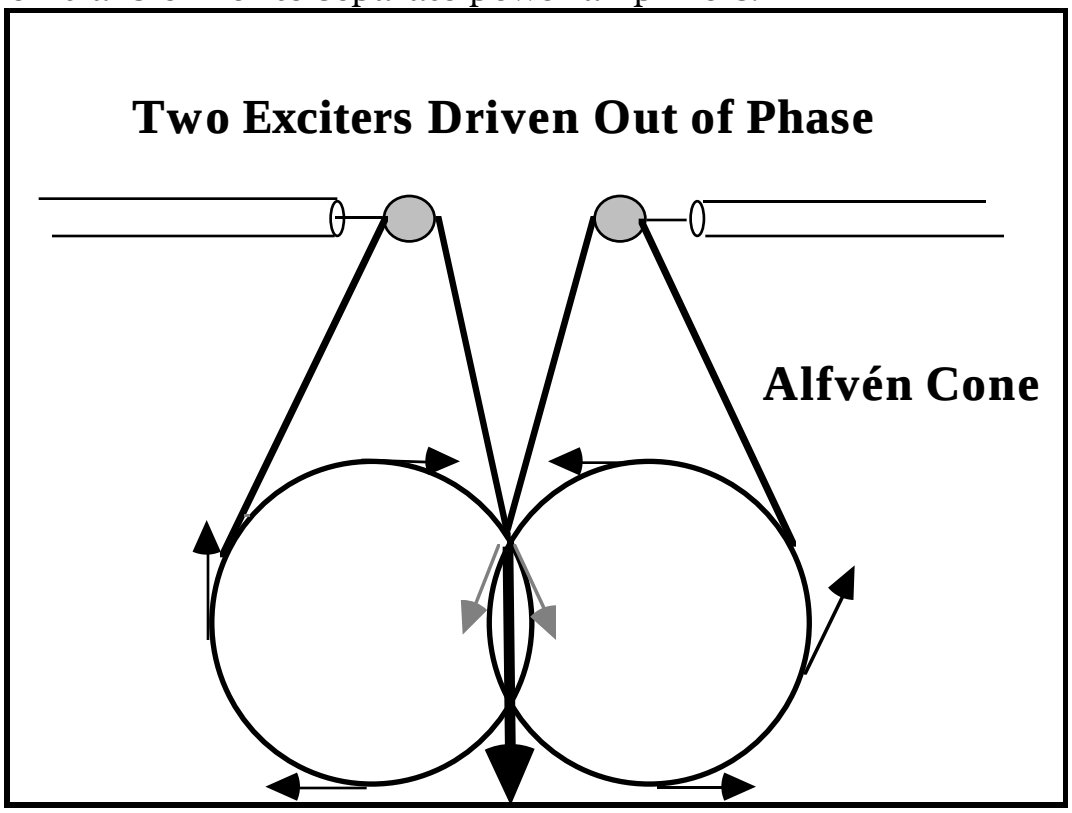

Figure8) Schematic illustrating two intersecting Alfvén cones. The interference pattern on axis produces an oscillating vertical field.

The amplitude and phase of the signals are controlled by an arbitrary waveform generator. The signal ground is referenced to an electrically floating Cu plate terminating the plasma column. The interaction of the waves was investigated at low and high wave currents. As discussed above small wave currents are obtained with the disks at floating potential because ion current is collected on half the RF cycle. Large wave currents are produced by biasing the disks positive and modulating the subsequent

electron saturation current. Antenna currents of several Amperes are easily attained using this technique.

The measured time-averaged wave magnetic field amplitude at low current is shown in Figure 9 for two different phasings of radiation at 200 kHz. The signals are in phase in Fig. 9a and 180 degrees out of phase in Fig. 9b. The two disks are one electron skin depth in radius (0.5 cm) and are separated by a distance of 6.3 cm across the magnetic field. The data plane is located 0.83 wavelengths (2.8 meters) from the disk exciters. When the exciters are driven in phase at the same amplitude there is a null in the wave magnetic field along a field line midway between them. The position of the null is a sensitive function of the phase difference between the exciters. The pattern appears to be that of a single exciter when the detector is positioned on field lines outside the flux tube containing the two disks. When the disk exciters are driven 180^{o} out of phase, a maximum is observed midway between them as shown in figure 9b. A comparison with theory for this case is presented in the lower figures 9c and 9d. The upper plane shown in Fig. 9 (a and b) is the experimental result while the lower plane (c and d) is a theoretical calculation of a linear superposition of the magnetic field radiated from each disk separately for the experimental parameters (B_0 = 1.0 kG, n = 2.0 $x10^{12}$ cm^{-3}, β_e = $2.5x10^{-4}$). In both cases one clearly sees the central maximum as well as two circular minima to the left and right of it. These minima are associated with the disk exciters but are not directly aligned along the magnetic field with them. The theoretically expected pattern closely matches the observed pattern.

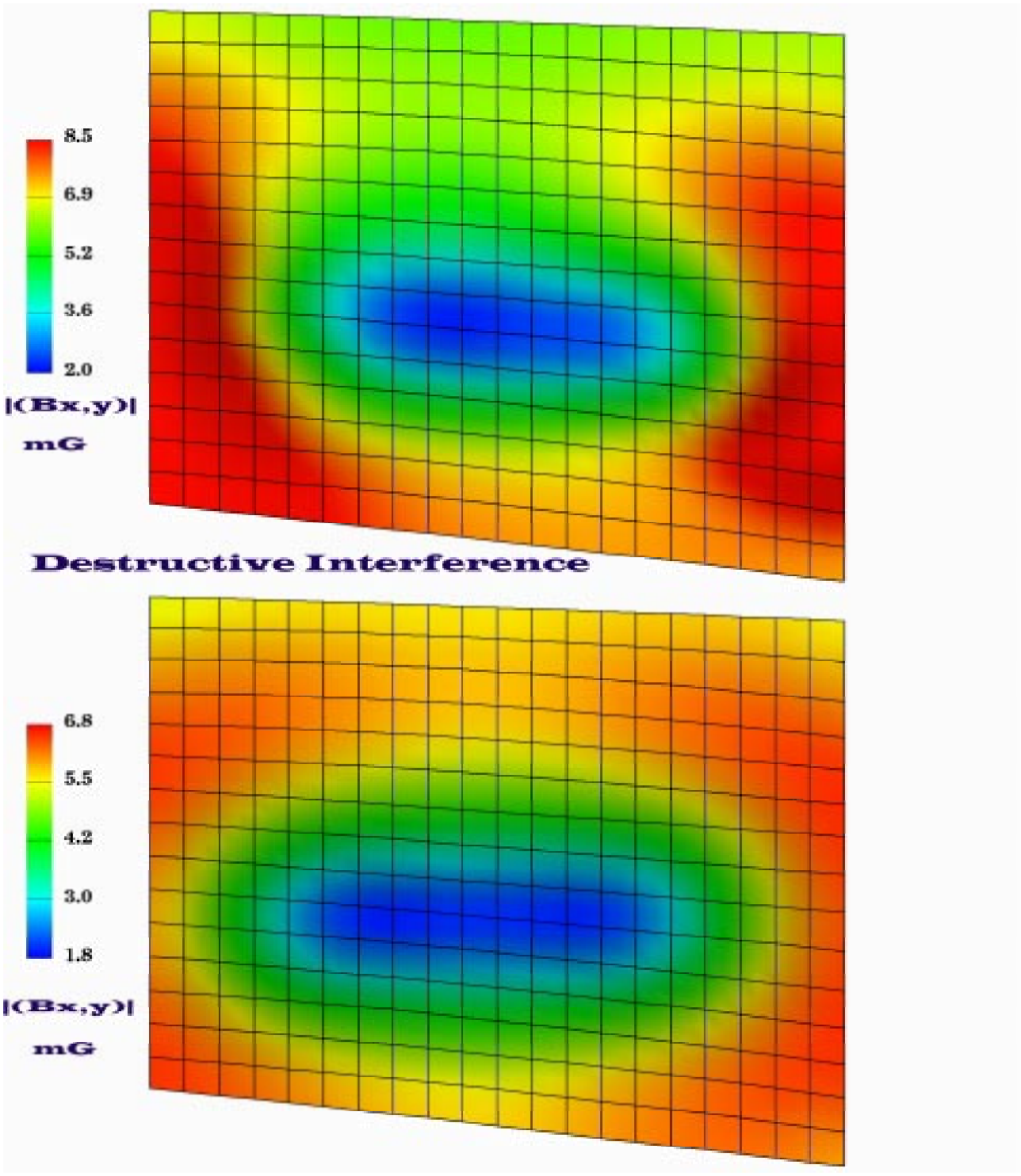

Figure 9a) Destructive interference of Alfvén wave cones. Experimental (upper plots) and theoretical wave patterns (lower plots) taken at δz = 2.8 meters from two disk exciters when they are driven in phase.

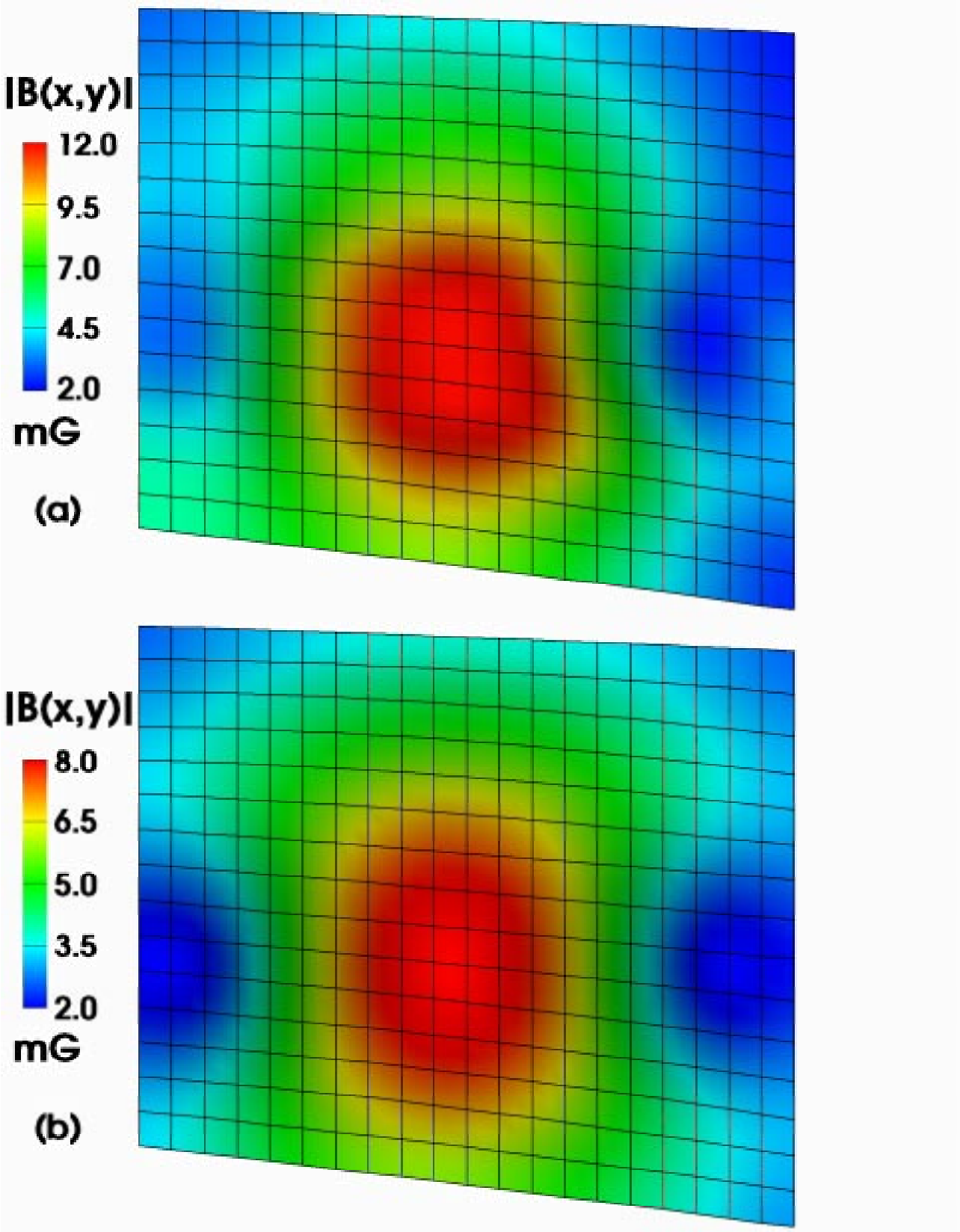
|B(x,y)|
12.0
9.5
7.0
4.5
2.0
mG
(a)
|B(x,y)|
8.0
6.5
5.0
3.5
2.0
mG
(b)

Figure9b) Constructive interference of Alfvén wave cones. Experimental (upper plots) and theoretical wave patterns (lower plots) taken at δz = 2.8 meters from two disk exciters when they are driven 180 degrees out of phase (right column). In the case of constructive interference the wave field is largest midway between the exiters. In both cases the exciters have radii of 0.5 cm (δ = 0.38 cm) and their separation across the field is 6.3 cm. The data grid is shown superposed, data was acquired at the intersection of the grid lines. The grid spacing is approximately 0.5 cm. Data was not acquired on a rectangular grid due to constraints on probe motion.

In the case of constructive interference the wave field is largest midway between the exiters and the exciters are driven 180 degrees out of phase. In both cases the exciters have radii of 0.5 cm (δ= 0.38 cm) and their separation across the field is 6.3 cm. The data grid is shown superposed, data was acquired at the intersection of the grid lines. The grid spacing is approximately 0.5 cm. Data was not acquired on a rectangular grid due to constraints on probe motion.

Large wave currents were obtained by applying a bias pulse of 28 Volts to both exciters 60 μsec before transmitting a 280 kHz, (ϖ = 0.67), five cycle tone burst. The antenna current was measured to be 11 Amps peak to peak. The antennas were separated by 3 cm across the magnetic field and driven 180^{o} out of phase. The background magnetic field was 1.1 kG, the plasma density 2.0 x 10^{12} cm^{-3}, and the plasma electron beta $2.3x10^{-4}$. A measured instantaneous value of the wave magnetic field is shown as a color coded surface in Figure 10. The axial component of the field is observed to be zero. The field midway between the exciters has a

maximum amplitude of 250 mG and is perpendicular to a line connecting the two antennas. In spite of the large antenna currents, there is no evidence for a nonlinear interaction, the resulting field pattern still appears to result from the linear superposition of the radiated field from each antenna. The parallel current is largest on and near the flux tubes containing the antennas. The subject of the three dimensional structure of the wave currents will be addressed in a subsequent paper.

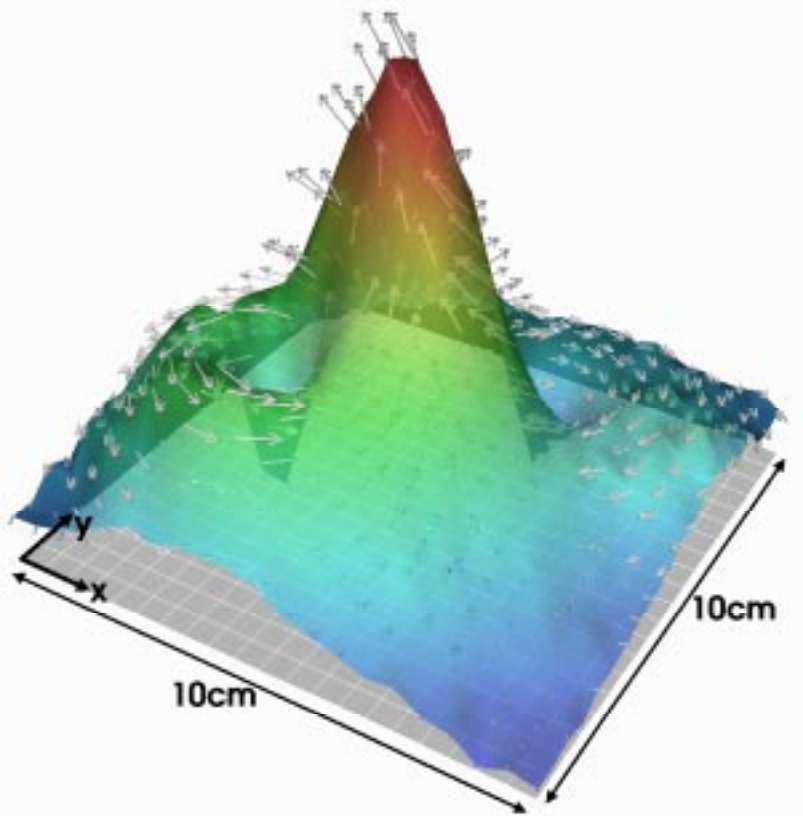

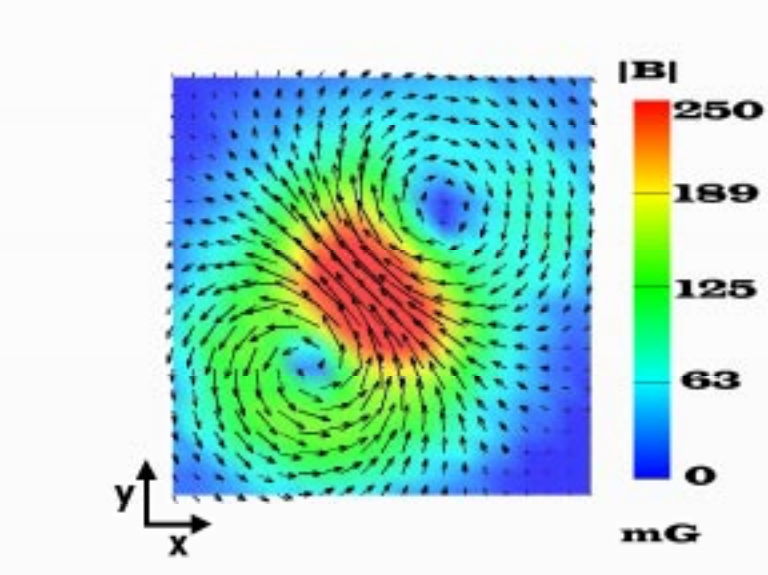

Figure 10) Magnetic field in the case of constructive interference of Alfvén wave cones. The magnitude is shown as a surface in (a) with an embedded vector field. For clarity the vectors are displayed in a view along the background magnetic field in (b).

V. Conclusions:

A series of laboratory experiments has been performed on the propagation of shear Alfvén waves which originate from sources with physical size across the magnetic field on the order of the electron skin depth. These small sources produce Alfvén wave patterns which contrast with the picture of standard MHD. This difference occurs as a result of corrections in the wave dispersion arising from non-zero perpendicular wave numbers ($k_\perp \delta \approx 1$). The inclusion of corrections arising from finite $k_\perp$ has two important consequences. Alfvén wave energy spreads across the magnetic field and the wave has a non-zero parallel electric field component. Spreading of magnetic energy implies that magnetic fluctuations associated with the shear Alfvén wave can be detected on field lines that do not directly connect with the source. On the other hand, the

parallel electric field component gives rise to the possibility that Alfvén waves can interact with particles leading to either wave growth or dissipation.

In the laboratory, we have verified by direct measurement the spreading of Alfvén wave energy across the magnetic field. For low beta plasmas (the so-called inertial Alfvén wave case) wave energy spreads along Alfvén wave cones which make an angle $\tan^{-1}(k_A\delta)$ with respect to the background field. This angle is typically very small, of order 1 degree. In higher beta plasmas (the so-called kinetic Alfvén wave case) wave energy also spreads across field lines in much the same fashion as for the low beta case, though strictly speaking, Alfvén wave cones do not exist for the kinetic Alfvén wave. We have indirectly verified the existence of the parallel electric field associated with the Alfvén wave by matching the observed profiles to theoretical predictions. These predictions depend upon the existence of collisionless dissipation (Landau damping) and its subsequent modification by electron pitch angle scattering. The observed profiles can not be fit unless these effects, which depend upon the existence of a parallel electric field component, are included.

The properties of Alfvén waves studied in the experiments reported here have several interesting consequences for the investigation of Alfvén waves in space plasmas. As far as Alfvén wave radiation is concerned small sources behave differently than large sources. Sources with fluctuating field aligned currents with scale sizes across the magnetic field on the order of the electron skin depth certainly exist in and around the magnetosphere. For example, the electron skin depth in the auroral ionosphere varies from several tens of meters at low altitudes to over a kilometer at altitude above 1 R_E. Features in the electron precipitation

associated with auroras are commonly observed (Borovsky, 1993) with cross field scale sizes in this range. If these currents have low frequency fluctuations they will radiate Alfvén waves that spread across field lines and have parallel electric field components.

The spreading of magnetic energy across field lines means that multiple current channels can interact giving fluctuations in the field not directly associated with a single source. For example, under the right conditions, constructive interference could produce regions of large, nonlocal, wave fields on field lines not directly connected to a current source. There is, therefore, a possible problem in interpreting the source of magnetic fluctuations detected by spacecraft if the source is a long distance away along the magnetic field. On the other hand, the parallel electric field associated with Alfvén waves radiated by small sources may lead to electron energization and field aligned fluxes of electrons. The sounding rocket observations by Boehm et al., (1990) of large amplitude Alfvén waves associated with density depressions and enhanced electron fluxes may be a manifestation of such an interaction.

The Freja observations in some sense complement those reported here. Freja was equipped with diagnostics that could measure the wave magnetic fields to extremely low frequencies (1-20 Hz) and had a electric dipole probe. Intense electromagnetic bursts with $(\frac{\Delta E}{\Delta B})c \approx V_A$ were observed with electromagnetic energy comparable to the background particle energy. These disturbances, classified as SKAW's dissipated rapidly in the non-homogeneous background plasma. These waves have also been observed in conjunction with ion acoustic turbulence (Wahlund et al 1994). In future work we will explore Alfvén wave cones at large amplitudes and see if they couple to density perturbations and give rise to electrostatic

noise. One possibility to achieve this in the laboratory is with the use of constructive interference. Clearly, in investigating possible sources and interactions of Alfvén waves in space plasmas consideration of effects arising from non-zero perpendicular wave number is of paramount importance.

Acknowledgements

We wish to thank the continual support of the Office of Naval Research who funded the contruction of the LAPD laboratory 10 years ago and the National Science Foundation. We also would like to acknowlege experimental contibutions by Alex Burke and Steve Rosenberg and the invaluable theoretical support of Prof. George Morales.

References

Alfvén, H., *Existence of electomagnetic-hydrodynamic waves*, Nature, **150**, 405 (1945)

Amagishi, Y., K. Saeki, I.J. Donnelly, *Excitation of MHD surfaces waves propagating with shear Alfvén waves in an inhomogeneous cylindrical plasma*, Plasma Phys. and Controlled Fusion, **31**, 675 (1989).

Amagishi, Y., *Experiments on mode conversion of m = -1 fast wave into a shear Alfvén wave in a cylindrical plasma*, J. Phys. Soc. of Japan, **59**, 2374 (1990).

Boehm, M.H., C.W. Carlson, J.P. McFadden, J.H. Clemmons, F.S. Mozer, *High-Resolution Sounding Rocket Observations of Large-Amplitude Alfvén Waves*, Jour. Geophys. Research, **95**, 12,157-12,171 (1990).

Borg, G.G., R.C. Cross, *Guided propagation of Alfvén andion-ion hybrid waves in a plasma with two ion species*, Plasma Phys. and Controlled Fusion, **29**, 681 (1987).

Borovsky, J.E., *Auroral Arc Thicknesses Predicted by Various Theories*, J. Geophys. Res., **98**, 6101-6138 (1993)

Bostick, W., M. Levine, *Experimental demonstration in the laboratory of the existence of magneto-hydrodynamic waves in ionized Helium*, Phys. Rev., **94**, 815 (1952).

Chmyrev, V.M., S.V. Bilichenko, O.A. Pokhotelov, V.A. Marchenko, V.I. Lazarev, A.V. Streltsov, L. Stenflo, *Alfvén Vorticies and Eelated Phenomena in the Ionosphere and the Magnetosphere,* Physica Scripta, **38** , 841-854 (1988).

Cross, R.C., J.A. Lehane, *Compressional Alfvén wave propagation below the ion cyclotron frequency*, Aust. J. Phys., **21**, 129 (1967a).

Cross, R.C., J.A. Lehane, *Propagation of compressional and torsional Alfvén waves under identical plasma conditions*, Nuclear Fusion, **7**, 219 (1967b).

Cross, R.C., *Experimantal observations of localized Alfvén and ion acoustic waves in a plasma*, Plasma Physics, **25**, 1377 (1983).

Gekelman, W., H. Pfister, Z. Lucky, J. Bamber, D. Leneman, J Maggs, *Design Construction and Properties of the Large Plasma Research Device-The LAPD at UCLA*, Rev. Sci. Instrum. **62**, 2875-2883 (1991).

Gekelman, W., D. Leneman, J. Maggs, S. Vincena, *Experimental Observation of Alfvén Wave Cones*, Phys. Plasmas, **1**, 3775-3785 (1994).

Jephcott, D.F., *Alfvén waves in a gas discharge*, Nature, **183**, 1652 (1959).

Jephcott, D.F., P.M. Stocker, *Hydrodynamic waves in a cylindrical plasma: An Experiment*, J. Fluid Mech, **13**, 587 (1962).

Koch, R.A., W. Horton Jr., *Effects of electron pitch angle scattering in plasma waves*, Phys. of Fluids, **18**, 861-865 (1975).

Lehane, J.A., F.J. Paoloni, *The propagation of non-axisymmetric Alfvén waves in an Argon plasma*, Plasma Physics, **14**, 701 (1971).

Louarn, P., J.E. Wahlund, T. Chust, H. de Feraudy, A. Roux, B. Holback, P.O. Dovner, A. I. Eriksson, G. Holmgren, *Observation of Kinetic Alfvén Waves by the Freja spacecraft*, Geophys. Research. Letts., **21**, 1847-1850 (1994).

Lundin, R., G. Haerendel, S. Grahn, *The Freja Project*, Geophys. Research. Letts., **21**, 1823-1826 (1994a).

Lundin, R., L. Eliasson, G. Haerendel, M. Boehm, B. Holback, *Large Scale Auroral plasma density cavities observed by Freja*, Geophys. Research. Letts., **21**, 1903-1096 (1994b).

Maggs, J. E., R. J. Taylor and W. Gekelman, *Neutral Burnout in a Ten Meter Liner Device*, Bull. Amer. Phys. Soc., 36, 2415 (1991).

Maggs, J.L, Morales, G.J, *Magnetic Fluctuations Associated with Field Aligned Striations*, Geophys. Res. Letts. 23, 633-636 (1996)

Morales, G.J., R.S. Loritsch, J.E. Maggs. *Structure of Alfvén Waves at the Skin-Depth Scale*, Phys. Plasmas, 1, 3765- (1994).

Müller, G., *Experimental Study of torsional Alfvén waves in a cylindrical partially ionized magnetoplasma*, Plasma Phys.,**16**, 813 (1973).

Sawyer, G.A., P.L. Scott, T. F. Stratton, *Experimental demonstrationof hydrodynamic waves in an ionized gas*, Phys. Fluids, **2**,47 (1959).

Wahlund, J.E., Louran, P., Churst, T., de Feraudy, H., Roux, A., Holbeck, B., Dovner, P-O., Holmgren, G. *On Ion Acoustic Turbulence and the Nonlinear Evolution of Kinetic Alfvén Waves in Aurora*, Geophys. Research, Letters, 21, 1831-1834 (1994)

Wilcox, J. M., F. I. Boley, A.W. De Silva*, Experimental study of Alfvén wave properties*, Phys. Fluids, **3**, 15 (1960).

Woods, L.C., *Hydrodynamic waves in a cylindrical plasma*, J. Fluid Mech., **13**, 570 (1962).